RESEARCH ARTICLE | JULY 08 2026

A tetrahedral probe constellation approach for measuring canonical momentum in self-organized laboratory plasma

C. C. Rouda ; A. M. Sellner ; J. von der Linden ; H. Himura ; R. Reksoatmodjo ; J. Sears ; S. You ; A. F. Almagri ; K. J. McCollam ; M. Reyfman ; J. S. Sarff

Rev. Sci. Instrum. 97, 075205 (2026)
https://doi.org/10.1063/5.0321458

Review of Scientific Instruments ARTICLE pubs.aip.org/aip/rsi

A tetrahedral probe constellation approach for measuring canonical momentum in self-organized laboratory plasma

Cite as: Rev. Sci. Instrum. 97, 075205 (2026); doi: 10.1063/5.0321458
Submitted: 7 January 2026 • Accepted: 6 June 2026 •
Published Online: 8 July 2026

View Online Export Citation CrossMark

C. C. Rouda,[1,a)] A. M. Sellner,[2] J. von der Linden,[3,4] H. Himura,[5] R. Reksoatmodjo,[6] J. Sears,[6] S. You,[2] A. F. Almagri,[1] K. J. McCollam,[1] M. Reyfman,[1] and J. S. Sarff[1]

AFFILIATIONS

[1] Department of Physics, University of Wisconsin-Madison, Madison, Wisconsin 53706, USA
[2] Helicityspace Corp., Pasadena, California 91107, USA
[3] Thea Energy, Inc., Kearny, New Jersey 07032, USA
[4] Max-Planck-Institute für Plasmaphysik, 85748 Garching, Germany
[5] Department of Electronics, Kyoto Institute of Technology, Kyoto 606-8585, Japan
[6] Lawrence Livermore National Laboratory, Livermore, California 94550, USA

[a)] **Author to whom correspondence should be addressed:** rouda@wisc.edu

ABSTRACT

To examine momentum redistribution processes and study generalized helicities during plasma relaxation in Madison Symmetric Torus, MST, reversed field pinch plasma, a new probe is being tested to measure the full 3D plasma ion flow and magnetic field vectors at four spatial locations arranged in a tetrahedral shape reminiscent of a satellite measurement constellation. These measurements permit calculation of $\nabla \times \vec{u}$ and canonical momentum, where $\vec{u}$ is the plasma ion flow vector. The probe consists of four probe heads arranged in a tetrahedral pattern, with an overall probe diameter of ~31.75 mm. The probe head diameter is ~1.0 cm, which is of the order of the ion Larmor radius. Each head has four molybdenum electrodes, also arranged in tetrahedral geometry, which are biased relative to a common return electrode, using four power supplies (one for each head), to measure the local ion flow. In addition, each head has three orthogonal magnetic pickup coils within it to measure equilibrium and fluctuating magnetic fields.

I. INTRODUCTION

Traditional relaxation models describe plasma self-organization in terms of single fluid models constrained solely by magnetic helicity.[1] Newer models show plasma relaxation as conversion between twisted magnetic flux tubes and twisted ion flow vorticity flux tubes. Magnetic flux tubes provide a framework for understanding self-organizational processes but are limited to static configurations.[2,3] This work provides the tools to study and generalize our understanding of canonical-helicity-constrained relaxation and to explain multi-scale dynamics. Fluid-helicity conservation and magnetic-helicity conservation are two limits of a more general conservation principle based on the helicity of canonical flux tubes. These tubes enclose a constant amount of flux of the canonical vorticity $\vec{\Omega}_\sigma$ and the curl of canonical momentum $\vec{P}_\sigma$,[3]

$$\vec{\Omega}_\sigma = \nabla \times \vec{P}_\sigma = n_\sigma(m_\sigma\vec{\omega}_\sigma + q_\sigma\vec{B}),$$

where σ denotes the species (i.e., electrons or ions), $\vec{u}_\sigma$ is the flow velocity, $\vec{\omega}_\sigma = \nabla \times \vec{u}_\sigma$ is the curl of the velocity, which is the flow vorticity, $\vec{B}$ is the magnetic field, n_σ is the species density, m_σ is the species mass, and q_σ is the species charge.

Understanding the energy conversion between flows and magnetic fields is an important frontier of plasma science. For example, the magnetic field of stars is sustained by 3D dynamo flows.[4] As these magnetic fields rise to the solar surface, they may reconnect, transferring magnetic energy to particle kinetic energy.[5] The accelerated particles can either cause an increase in electromagnetic radiation in the form of flares or eject from the stars as a coronal jet or coronal mass ejection.[6,7]

Previous work in linear screw pinches using multi-point measurements with internal Mach[8] and B-dot probes using ensembles from many shots showed that canonical helicity was conserved but magnetic helicity was not.[9] In toroidal experiments such as tokamak and reversed field pinch (RFP) plasmas, which use inductively driven current, diagnostic access is limited, precluding dense probe coverage throughout the volume.

Many experiments studying reconnection events have been conducted in MST, where it has been observed that sawteeth are the result of nonlinear coupling in m = 1 tearing modes.[10] During sawtooth relaxation processes, fluctuations on two-fluid scales[11] redistribute parallel current density profiles.[12–16] Capacitive probes have measured a radially inward pointing electric field during sawtooth crashes.[17] Magnetic fluctuations' measurements have shown that non-linear coupling in m = 1 modes leads to momentum transport driven by the Hall dynamo term.[14,18] To determine whether this new model more accurately describes self-organization when including both flows and magnetic measurements, a probe capable of both 3D measurements and the ability to measure ion velocity $\vec{u}_I$ and calculate vorticity $\vec{\omega}_I$ (to account for two fluid effects[11,12]) is needed.

Here, we pursue a probe design reminiscent of cluster spacecraft missions flying in tetrahedral arrangements,[19,20] sometimes called constellations.[21] These missions have calculated flow vorticity by constructing numerical estimates of the curls from the species flows measured with electrostatic analyzers. For instance, a prominent geometric curl estimator uses a Stokes integral method for a tetrahedral array of measurements.[21] Our probe's approach is double tetrahedral, i.e., the geometric advantage is applied for both the Mach measurement of the plasma flow as well as fluid vorticity using four identical heads. While a similar tetrahedral array probe for electrostatic and magnetic measurements was used previously on the Madison Symmetric Torus, MST,[22] for magnetic helicity injection studies,[23] to the best of our knowledge, such a constellation approach for plasma flow and vorticity has not been deployed in a laboratory setting. It minimizes the number of Mach electrodes required to measure local fluid vorticity.

The newly developed tetrahedral constellation probe can measure these fluxes simultaneously during plasma relaxation processes. The probe consists of four clusters of B-dot coils and Mach probes, each measuring the local 3D vectors of magnetic field and ion flow. The 3D Mach vector is determined by a matrix method that includes the 3D angles of the tips.[24] The four clusters are arranged in a tetrahedral geometry. The probe has been constructed and tested on MST during sawtooth relaxation. Section II covers our probe design. In Sec. III, we describe the electronics used and their calibration. In addition, in Sec. IV, we show raw probe data from MST plasma discharges.

II. PROBE THEORY AND DESIGN

The tetrahedral constellation probe consists of four stalks arranged to allow measuring $\nabla \times \vec{u}$. To develop our designs, we built and tested two prototype probes[25,26] with a single cluster of B-dot coils and Mach electrode tips.[8] The first prototype[25] was a single stalk Mach probe with six molybdenum tips arranged in an octahedral geometry. A full probe designed from this prototype with six fingers would have been too large to fit in the 38.1 mm diameter MST port hole so a second prototype with tetrahedral geometry was created. The change in geometry allowed us to reduce the overall size of the final probe. The second prototype was a single stalk probe with four Mach tips arranged in a tetrahedron, as enabled by a generalized

FIG. 1. Image of the completed tetrahedral Mach probe with four stalks, with molybdenum tips in place and the return electrode ring at the bottom.

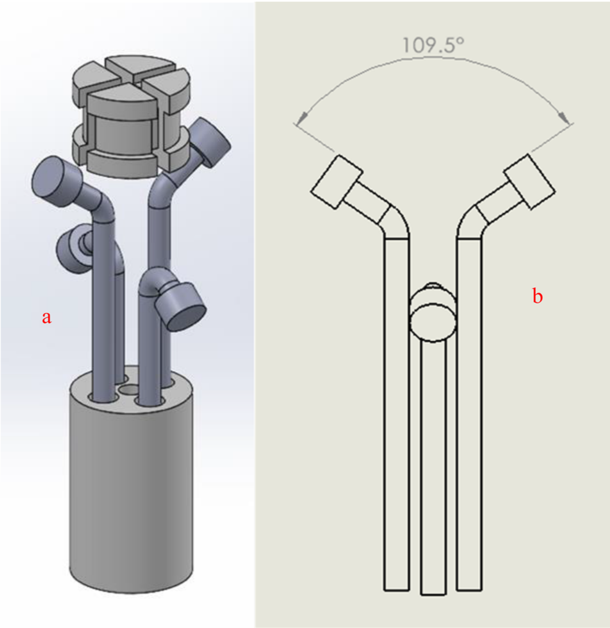

FIG. 2. (a) Drawing of internal components of a single stalk containing the internal spacer to keep moly tips in correct configuration and at the location of the B-Dot coil. Panel (b) shows tetrahedral angle between each two tips.

Mach probe analysis method.[24] After the successful testing of the single stalk tetrahedral Mach probe prototype, the probe described in this work was designed and constructed as a four-stalk tetrahedral Mach probe array, as shown in Fig. 1. The full tetrahedral Mach probe has an overall diameter of ~31.75 mm.

Each stalk of the full probe houses three magnetic orthogonal pickup coils and four molybdenum tips arranged in a tetrahedral configuration. Each tip is biased negative relative to a 31.75 mm diameter electrode ring on the base of the probe, which serves as a return electrode for all 16 electrode tips (Fig. 1). To collect ion saturation current, each array of four tips functions as a novel Mach probe to measure 3D plasma ion flow velocity. In traditional 1D upstream/downstream Mach probes,[9] the flow to be measured is related to the ratio of ion saturation currents for the two opposing tips,

$$M = \left(\frac{1}{K}\right) \ln\left(I_{upstream}/I_{downstream}\right),$$

where $M = u/c_s$ is the Mach number for the ion flow speed u and ion sound speed c_s, and K is a calibration constant that depends on the plasma model. However, with our tetrahedral Mach probe, there are no directly opposing tips, and a more complex matrix algorithm accounting for the tip angles is needed, which is detailed in Ref. 24.

Each individual Mach probe stalk has two obtuse tips (bent at 125.26°) and two acute tips (bent at 54.74°); see Fig. 2. The tips are configured to form a tetrahedron with an angle of 109.5° between each two tips. Each tip has a collection area of 3.14 mm^2 to limit the collected ion saturation current from ohmic heating internal components after a repeated large number of plasma discharges. The molybdenum tips have a 0.381 mm diameter and a 6 mm deep hole at the bottom for the central conductor of a 32 AWG (0.2 mm diameter) Kapton-insulated coaxial cable that slides into and is then crimped. The molybdenum tips do not protrude beyond the probe face. The tips are held in place and isolated from each other with a boron nitride, BN, spacer and extended through the BN probe head until only the collection area is exposed. The probe head diameter is 10.16 mm, which is of the order of the ion Larmor radius. Each Mach probe also contains three orthogonal magnetic pickup coils. Each bobbin sits above the tips. The pickup coils used to measure the transverse components of the magnetic field (toroidal or poloidal) have effective areas of 85 and 65 mm^2, and the pickup coil used for the radial component of the magnetic field has an effective area of 200 mm^2. The two transverse coils with areas depending on probe rotation during experiments on these coils would measure either the toroidal or poloidal magnetic field.

The collected ion saturation current is measured via a network of resistors (see Sec. III). During experiments, the probe was

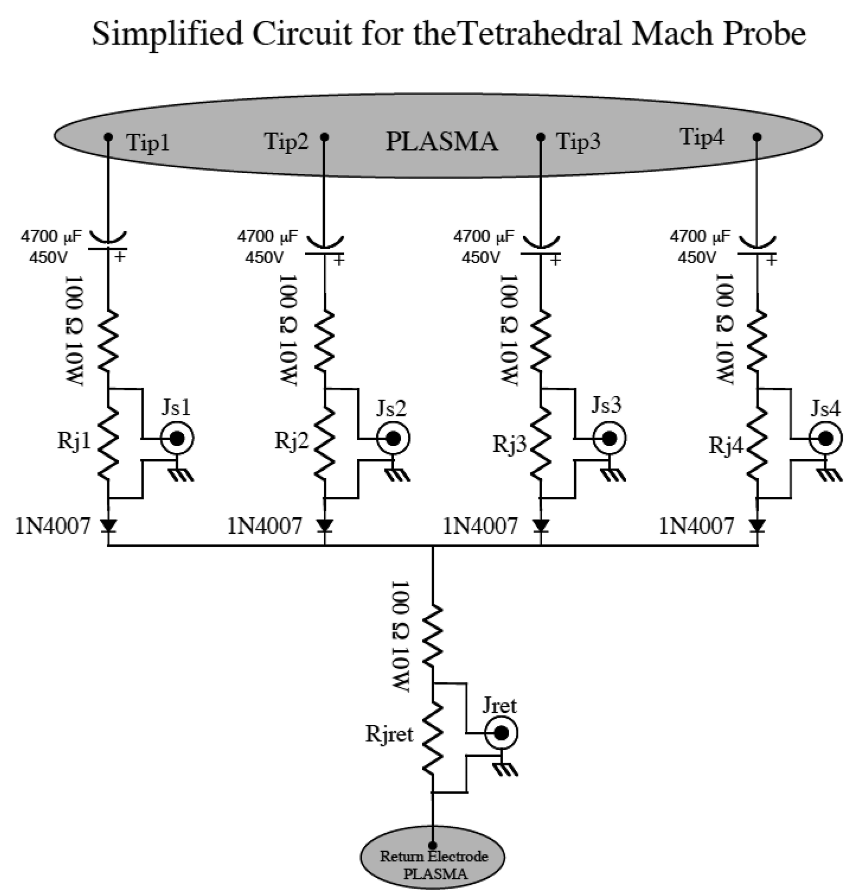

FIG. 3. Simplified circuit diagram of the electrode (tips 1–4) biasing. Capacitors are continually charged to an adjustable voltage of up to 450 V via an isolation transformer (not shown) and the tips are biased negative with respect to the return electrode. Digitizers, connected through isolation amplifiers, record the current as the voltage across the resistors for each electrode Rj1–Rj4 and the return Rjret.

inserted into the plasma up to $r/a \approx 0.85$, where r and a are the radial location of the leading Mach stalk and the plasma radius, respectively.

III. ELECTRONICS AND CALIBRATION

Each of the four versatile power supplies used to bias the Mach probe tips consists of seven channels, six inputs for the probe tips and one output for the return current. Four power supplies are used with the tetrahedral Mach probes, one for each head. Only four of the available six channels are used in each supply. The return currents from each head are summed together to provide a measurement of the total return electrode current.

Each power supply has the capacity to work with up to a six-tip version of a Mach probe. As shown in simplified form in Fig. 3, each channel has a corresponding resistive divider to optimize the current measurements. The resistive divider contains one 100 Ω resistor and a second resistor (R_j), which can be adjusted to 1, 2, 5,10, 20, 50, and 100 Ω and allows the power supplies to be used on probes with different collection areas or plasmas with different parameters. The tips are biased negative with respect to the return electrode to ~150 V (which is $\geq 3T_e$, where T_e equals 30–40 eV) using 4700 μF electrolytic capacitors to ensure the tips are in the ion saturation current regime.[27] The bias voltage is essentially constant since the 4700 μF capacitor is in series with 200 Ω resisters, resulting into an RC = 940 ms, which is over 20 times longer than the discharge duration. The voltage of each capacitor is monitored by a voltmeter. All 16 measured ion saturation currents are connected to a 150 kHz isolation amplifier before being digitized.

The ion saturation current for each tip, $I_{sat,j}$, is related to the measured voltage, V_j across the corresponding R_j resistor as $V_j = R_j * I_{sat,j}$. To calibrate the resistive network divider, a 1 kΩ (with 1% uncertainty) resistor load is connected between each tip and the return electrode to act as a plasma load. The current through the 1 kΩ resistor is measured to determine the actual R_j values used to calculate I_{sat}. For the plasmas discussed here, the tips operate in the unmagnetized regime. In addition, the tips are designed to have the same collecting area. The procedure converting the ion saturation current measurements in tetrahedral geometry into the local plasma flow is described in Ref. 24.

There are four triaxial magnetic pickup coils that are calibrated in two different ways. The first method uses a Helmholtz coil driven by a signal generator where each pickup coil output is measured as a function of frequency to determine the coil effective area and frequency bandwidth. The second method is by using MST vacuum toroidal field which is accurately known. The response of each coil to the vacuum toroidal field is integrated with an active integrator with $RC = 10^{-4}$ s and variable secondary gain, G. The coil effective area is given by

$$A(m^2) = \frac{V_C(\text{volts}) * RC(s)}{G * BT(\text{tesla})},$$

where BT (tesla) is the vacuum toroidal field and V_C (volts) is the integrator output signal from the magnetic coil. The areas of the two non-radial coils, Coil 1 and Coil 2, are calculated both by using MST vacuum field and Helmholtz, which produce a similar effective area. The area of the radial coil is calculated using solely the Helmholtz coil method. The Helmholtz coil calibration also allows for determining the frequency responses of all the coils.

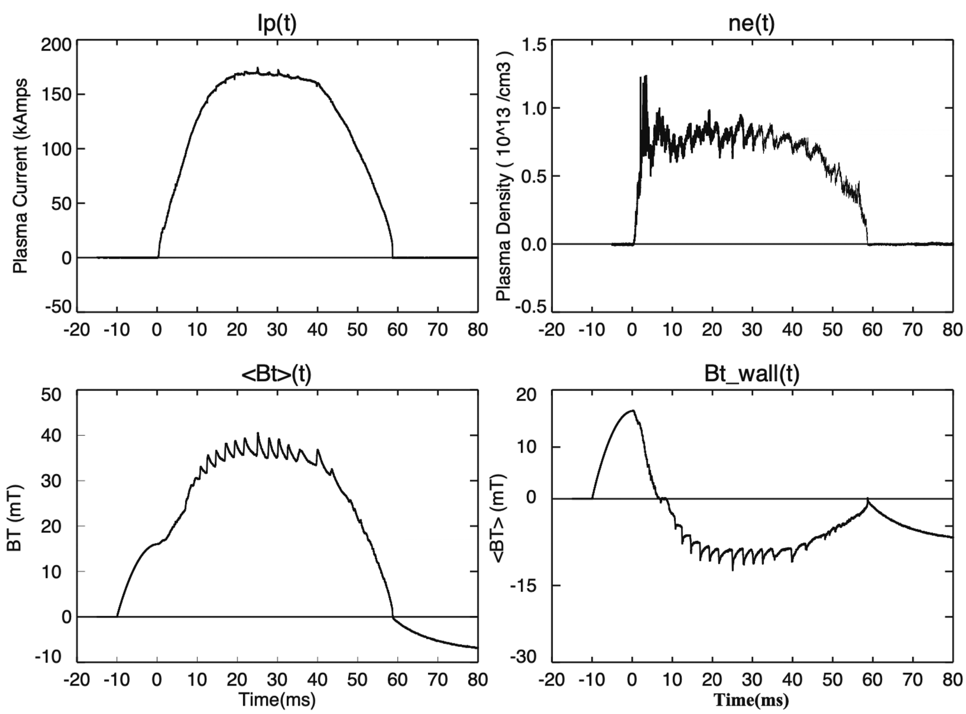

FIG. 4. Plasma parameters during typical shots. The top left panel shows plasma current of $I_P = 170 \pm 4$ kA. The top right panel shows plasma density $n_e = 0.8 \pm 0.02 \times 10^{19}$ m^{-3}. The bottom left panel shows the average toroidal magnetic field $\langle B_T \rangle$. The bottom right panel shows the toroidal magnetic field measured at the conducting shell $B_T(a)$.

The measured effective areas of all the coils are independent of frequency in the frequency range of up to 150 kHz. The integrator has a 250 kHz bandwidth, and all signals are digitized at 1 MHz. The dominant magnetic fluctuations in the plasmas discussed in the following arise from tearing instability with temporal dynamics <150 kHz.

IV. DATA AND EXPERIMENTAL RESULTS

The probe was inserted into the MST device during RFP plasma discharges, with parameters shown in Fig. 4. The plasma current was $I_P = 170 \pm 4$ kA lasting 35 ms, as shown in Fig. 4(a). Plasma density during flattop was $n_e = 0.8 \pm 0.02 \times 10^{19}\ \mathrm{m}^{-3}$, as shown in Fig. 4(b).

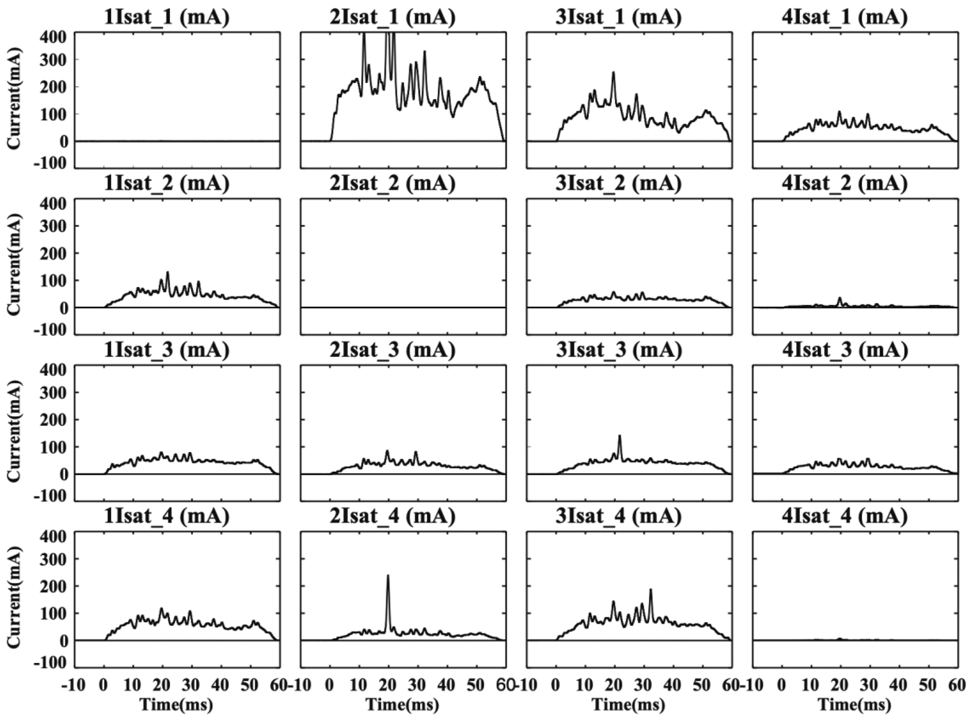

FIG. 5. Collected ion saturation currents from all 16 tips during a typical shot. 1Tip_1, 2Tip_2, 4Tip_2, and 4Tip_4 were disconnected. The return electrode current (see Fig. 7) agrees well with the sum of the individual tips.

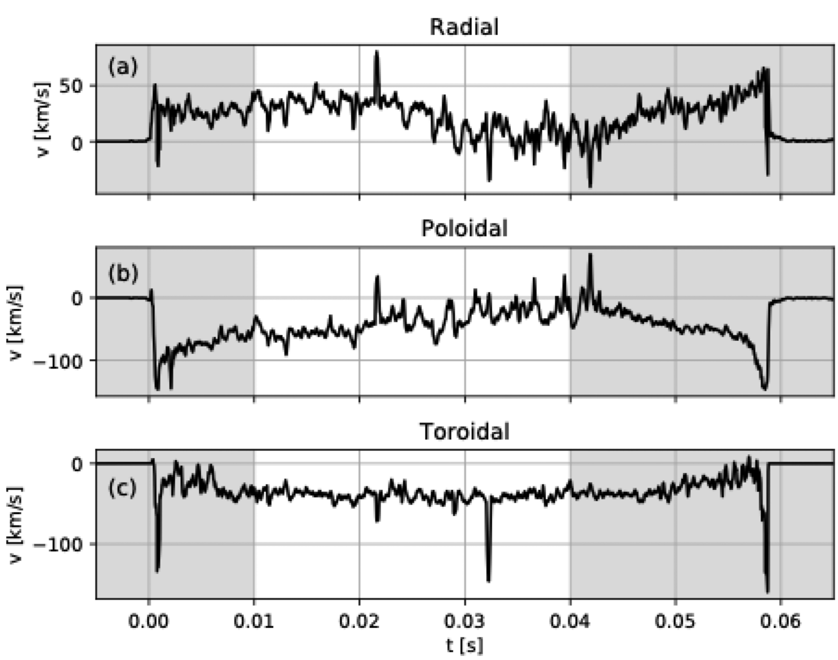

FIG. 6. Preliminary velocity waveforms based on ion saturation currents measured with probe stalk 3. (a) Radial component; positive means outward. (b) Poloidal component; positive means toward outboard on top. (c) Toroidal component; positive means counterclockwise viewed from top. The white background indicates the plasma flattop period, and the gray backgrounds indicate the plasma startup and rampdown.

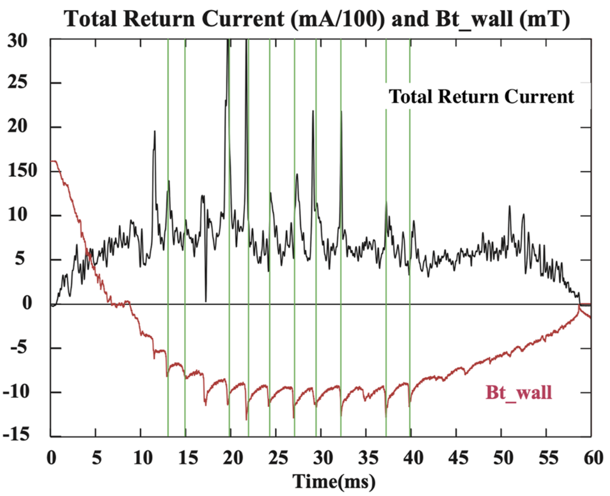

FIG. 7. Toroidal field at the wall ($Bt_{\_wall}$ in red) and current through return electrode I_{return}. The dashed gray lines mark the time that the sawtooth crashes in $Bt_{\_wall}$.

The probe was inserted to $r/a = 0.9$, where $r = 47$ cm and $a = 52$ cm is the MST minor radius. During flattop, the reversal surface, r_s, was at $0.82 < r_s/a < 0.84$ as previously measured by magnetic probes.[28] Figure 4(c) shows the average toroidal magnetic field $\langle B_\phi \rangle$, and Fig. 4(d) shows the toroidal magnetic field measured at the conducting shell $B_\phi(a)$. The plasma core temperature is about 100 eV. The probe's molybdenum tips and the boron nitride (BN) surfaces underwent multiple nights of conditioning using pulsed discharge cleaning (PDC) to reduce the sputtering of fresh probe surfaces due to plasma interaction.

The ion saturation currents collected by the 16 molybdenum tips are shown in Fig. 5. For the purpose of probe orientation, the four stalks are labeled 1 through 4 and the corresponding tips are labeled with two digits (n Tip_m), where n = 1, 2, 3, 4 corresponds to the stalk number and m = 1, 2, 3, 4 corresponds to the tip position, such that tips (1 Tip_1), (1 Tip_2), (1 Tip_3), and (1 Tip_4) are all in Stalk 1. The odd numbered tips are bent at obtuse angles, and the even numbered tips are bent at acute angles. The odd numbered stalks are longer than the even numbered stalks, such that the four heads are in a tetrahedral configuration, as shown in Sec. II. Four of the tips were accidentally disconnected from the coaxial cable during assembly, (1 Tip_1), (2 Tip_2), (4 Tip_2), and (4 Tip_4), which prevented the complete set of flow measurements needed to evaluate the vorticity. Once the electrodes are conditioned, the ion saturation current exhibits a rise to a plateau during the plasma discharge. This plateau is consistent with measurements from the octahedral prototype reported by Sellner *et al.*[25]

The measured ion saturation currents from Stalk 3 were used to produce preliminary 3D velocity waveforms shown in Fig. 6. These velocity components for the radial, poloidal, and toroidal directions were calculated using a matrix analysis method detailed in Ref. 24. To the best of our knowledge, this and similar results shown in Ref. 24 are the first successful measurements of the local 3D ion flow in a laboratory plasma using only four electrodes in a

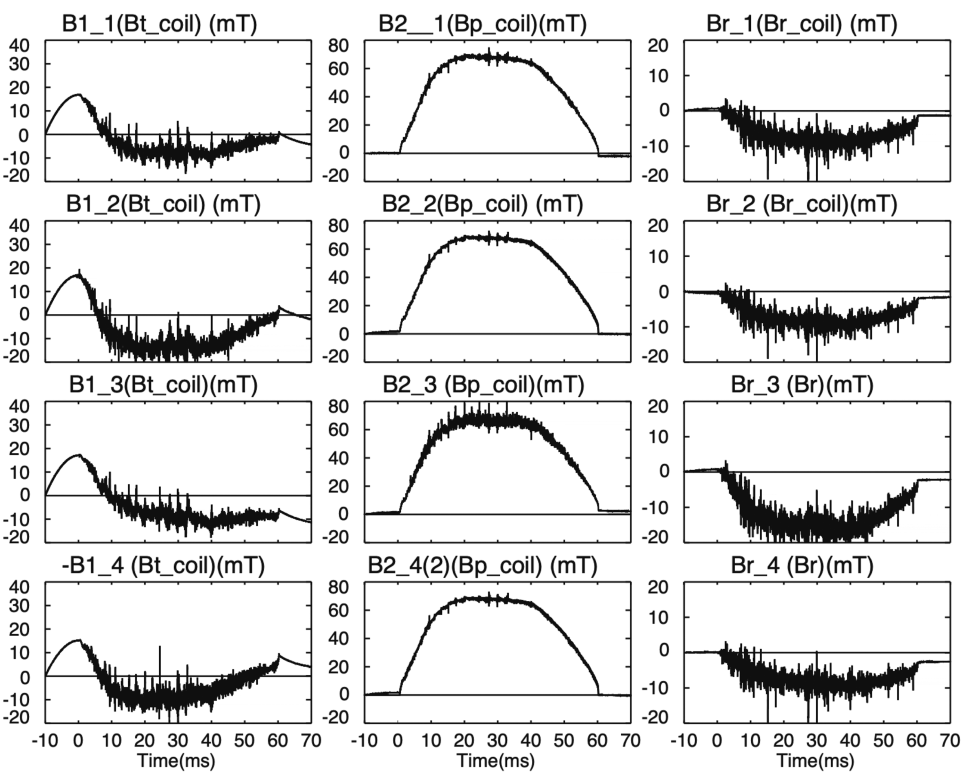

FIG. 8. Magnetic field measurements from each triaxial magnetic pickup coil. Column one shows the poloidal magnetic field; column two shows the Toroidal magnetic field; and column 3 shows the radial magnetic field.

tetrahedral arrangement. The results are preliminary but have the expected overall order of magnitude and have some points of agreement with previous MST results from a 2D Mach probe.[29]

Procedures for estimating the curl of a local vector field, $\vec{A}$, using measurements in tetrahedral formation are well established. The approach described in Ref. 21 employs Stokes theorem,

$$\int_V \nabla \times \vec{A}\ dV = \oint_S d\vec{S} \times \vec{A}$$

to make the estimator,

$$\langle \nabla \times \vec{A} \rangle = \frac{1}{V} \sum_{i=1}^{4} \vec{S}_i \times \langle \vec{A} \rangle_i,$$

where angle brackets $\langle \cdots \rangle$ are appropriate averages over the tetrahedral volume, V, and $\vec{S}_i$ represents four vectors normal to the tetrahedral faces with magnitudes equal to the face areas. With $\vec{A} = \vec{u}_\sigma$ (the local plasma flow velocity), this procedure would have yielded the fluid vorticity $\vec{\omega}_\sigma = \nabla \times \vec{u}_\sigma$.

Figure 7 shows sawteeth features in the total return current (black). The total return current shows an increase in the collected ion saturation currents by the molybdenum tips at the sawtooth crashes that may be consistent with redistribution of plasma flow profile at reconnection events, but further analysis of a radial scan with flux surface averaging would be needed to confirm that this is true. Time correlation of the increase in ion saturation currents with the sawteeth in the toroidal field at the wall (red) will also be the topic of future research.

Probe measurements of the magnetic fields are shown in Fig. 8. Edge measurements of the toroidal magnetic field are negative, as expected, as it is outside the reversal surface. The poloidal magnetic field has a waveform of a similar shape as the plasma current. The sawteeth and high frequency fluctuations only appear in the toroidal and radial magnetic fields.

V. CONCLUSION

A novel tetrahedral 3D Mach B-dot probe arranged similarly to a satellite constellation has been designed and tested in MST RFP laboratory plasmas. The constituent tetrahedral probes produce reasonable ion saturation current measurements consistent with previous MST results from 2D-Mach probes.[10,18] This represents the first successful measurement of local 3D ion flow using a tetrahedral Mach tip arrangement by applying a novel matrix method described in Ref. 24. Unfortunately, the loss of four critically located tips out of sixteen total tips prevented a measurement of the curl of the ion flow velocity and the canonical vorticity. The mechanical/electrical connection of lead wires to the molybdenum tips could be made more robust using precision vacuum brazing in future probe designs.

ACKNOWLEDGMENTS

The experiments were conducted at the Wisconsin Plasma Physics Laboratory (WiPPL), a research facility supported by the DOE Office of Fusion Energy Sciences under Award No. DE-AC52-07NA27344 (LLNL) and Contract No. DE-SC0018266 with major facility instrumentation developed with support from the National Science foundation under Award No. PHY1828159. This article is dedicated to the memory of Peter J. Weix, a senior technician on MST. He will be missed.

AUTHOR DECLARATIONS

Conflict of Interest

The authors have no conflicts to disclose.

Author Contributions

C. C. Rouda: Data curation (lead); Investigation (lead); Methodology (lead); Resources (lead); Writing – original draft (lead); Writing – review & editing (lead). **A. M. Sellner**: Data curation (equal); Investigation (equal); Methodology (equal); Resources (equal). **J. von der Linden**: Conceptualization (lead); Formal analysis (equal); Funding acquisition (equal); Investigation (equal); Methodology (equal); Project administration (equal); Visualization (equal); Writing – review & editing (equal). **H. Himura**: Formal analysis (equal); Methodology (equal); Writing – review & editing (equal). **R. Reksoatmodjo**: Formal analysis (equal); Methodology (equal); Writing – review & editing (equal). **J. Sears**: Project administration (equal); Writing – review & editing (equal). **S. You**: Conceptualization (equal). **A. F. Almagri**: Investigation (equal); Methodology (equal); Writing – original draft (equal); Writing – review & editing (equal). **K. J. McCollam**: Formal analysis (equal); Project administration (equal); Validation (equal); Writing – review & editing (equal). **M. Reyfman**: Methodology (equal). **J. S. Sarff**: Supervision (equal); Writing – review & editing (equal).

DATA AVAILABILITY

The data that support the findings of this study are available from the corresponding author upon reasonable request.

REFERENCES

[1] J. B. Taylor, Phys. Rev. Lett. **33**, 1139 (1974).
[2] L. C. Steinhauer and A. Ishida, Phys. Rev. Lett. **79**, 3423 (1997).
[3] S. You, Phys. Plasmas **23**, 072108 (2016).
[4] Y. Fan, "Magnetic fields in the solar convection zone," Living Rev. Sol. Phys. **1**, 1 (2004).
[5] M. I. Desai, J. F. Drake, T. Phan, Z. Yin, M. Swisdak, D. J. McComas, S. D. Bale, A. Rahmati, D. Larson, W. H. Matthaeus, *et al.*, Astrophys. J. Lett. **985**, L38 (2025).
[6] T. Howard, *Coronal Mass Ejections: An Introduction*, *Astrophysics and Space Science Library* (Springer, New York, 2011), Vol. 376.
[7] P. F. Chen, "Coronal mass ejections: Models and their observational basis," Living Rev. Sol. Phys. **8**, 1 (2011).
[8] K.-S. Chung, "Mach probes," Plasma Sources Sci. Technol. **21**, 063001 (2012).
[9] T. DeHaas and W. Gekelman, Phys. Plasmas **24**, 072108 (2017).
[10] T. D. Tharp, A. F. Almagri, M. C. Miller, V. V. Mirnov, S. C. Prager, J. S. Sarff, and C. C. Kim, Phys. Plasmas **17**, 120701 (2010).
[11] J. R. King, C. R. Sovinec, and V. V. Mirnov, Phys. Plasmas **19**, 055905 (2012).
[12] H. Ji, S. C. Prager, and J. S. Sarff, Phys. Rev. Lett. **74**, 2945 (1995).
[13] J. K. Anderson, C. B. Forest, T. M. Biewer, J. S. Sarff, and J. C. Wright, Nucl. Fusion **44**, 162 (2003).
[14] A. Kuritsyn, G. Fiksel, A. F. Almagri, D. L. Brower, W. X. Ding, M. C. Miller, V. V. Mirnov, S. C. Prager, and J. S. Sarff, Phys. Plasmas **16**, 055903 (2009).

[15] J. P. Sauppe and C. R. Sovinec, Phys. Plasmas **23**, 032303 (2016).
[16] J. C. Triana, "Measurements of two-fluid relaxation in the Madison symmetric torus," Ph.D. thesis, University of Wisconsin-Madison, 2017.
[17] M. Tan, D. R. Stone, J. C. Triana, A. F. Almagri, G. Fiksel, W. Ding, J. S. Sarff, K. J. McCollam, H. Li, and W. Liu, Rev. Sci. Instrum. **88**, 023502 (2017).
[18] A. Kuritsyn, G. Fiksel, M. C. Miller, A. F. Almagri, M. Reyfman, and J. S. Sarff, Rev. Sci. Instrum. **79**, 10F127 (2008).
[19] G. Paschmann and P. Daly, *Analysis Methods for Multi-Spacecraft Data* (ESA Publications Division, 1998).
[20] R. Kieokaew, C. Foullon, and B. Lavraud, J. Geophys. Res.: Space Phys. **123**, 513, https://doi.org/10.1002/2017ja024424 (2018).
[21] C. Shen and M. Dunlop, "Field gradient analysis based on a geometrical approach," J. Geophys. Res.: Space Phys. **128**(6), e2023JA031313, https://doi.org/10.1029/2023ja031313 (2023).
[22] R. N. Dexter, D. W. Kerst, T. W. Lovell, S. C. Prager, and J. C. Sprott, "The Madison symmetric torus," Fusion Technol. **19**(1), 131–139 (1991).
[23] D. R. Stone, "Magnetic relaxation during oscillating field current drive in a reversed field pinch," Ph.D. thesis, University of Wisconsin-Madison, 2013.
[24] K. J. McCollam, R. Reksoatmodjo, J. von der Linden, J. Sears, S. You, H. Himura, A. F. Almagri, M. Reyfman, C. C. Rouda, J. S. Sarff, and A. M. Sellner, "Three-dimensional unmagnetized Mach probe analysis and initial flow measurements in reversed-field pinch experiments," arXiv:2510.14212 [physics.plasm-ph] (2025).
[25] A. M. Sellner, J. von der Linden, H. Himura, R. Reksoatmodjo, J. Sears, S. You, A. F. Almagri, K. J. McCollam, M. Reyfman, C. C. Rouda, and J. S. Sarff, "An octahedral Mach B-dot probe for 3D flows and magnetic fields in the edge of reversed field pinches," Rev. Sci. Instrum. **95**, 073536 (2024).
[26] H. Himura, A. F. Almagri, J. S. Sarff, Y. Ashida, S. Inagaki, H. Fujiwara, T. Inoue, A. Sanpei, J. von der Linden, K. J. McCollam, N. C. Hurst, and C. B. Forest, "All-in-one probe for exploring self-organized two-fluid equilibria in toroidal plasmas," Rev. Sci. Instrum. **95**(8). 083537 (2024).
[27] X. Zhang, D. Dandurand, T. Gray, M. R. Brown, and V. S. Lukin, Rev. Sci. Instrum. **82**, 033510 (2011).
[28] V. Antoni, D. Merlin, S. Ortolani, and R. Paccagnella, Nucl. Fusion **26**, 1711 (1986).
[29] M. Miller, "Non-axisymmetric flows and transport in the edge of MST," Ph.D. thesis, University of Wisconsin-Madison, 2011.